

ELECTROMAGNETIC MODELLING AND SIMULATION OF A HIGH-FREQUENCY GROUND-PENETRATING RADAR ANTENNA OVER A CONCRETE CELL WITH STEEL RODS

ALESSIO VENTURA (CORRESPONDING AUTHOR) & LARA PAJEWSKI

DEPARTMENT OF INFORMATION ENGINEERING, ELECTRONICS AND TELECOMMUNICATIONS,
SAPIENZA UNIVERSITY OF ROME, ROME, ITALY
ALESSIOVENTURA@HOTMAIL.COM, LARA.PAJEWSKI@UNIROMA1.IT

ABSTRACT

This work focuses on the electromagnetic modelling and simulation of a high-frequency Ground-Penetrating Radar (GPR) antenna over a concrete cell with reinforcing elements. The development of realistic electromagnetic models of GPR antennas is crucial for accurately predicting GPR responses and for designing new antennas. We used commercial software implementing the Finite-Integration technique (CST Microwave Studio) to create a model that is representative of a 1.5 GHz Geophysical Survey Systems, Inc. antenna, by exploiting information published in the literature (namely, in the PhD Thesis of Dr Craig Warren); our CST model was validated, in a previous work, by comparisons with Finite-Difference Time-Domain results and with experimental data, with very good agreement, showing that the software we used is suitable for the simulation of antennas in the presence of targets in the near field. In the current paper, we firstly describe in detail how the CST model of the antenna was implemented; subsequently, we present new results calculated with the antenna over a reinforced-concrete cell. Such cell is one of the reference scenarios included in the Open Database of Radargrams of COST Action TU1208 “Civil engineering applications of Ground Penetrating Radar” and hosts five circular-section steel rods, having different diameters, embedded at different depths into the concrete. Comparisons with a simpler model, where the physical structure of the antenna is not taken into account, are carried out; the significant differences between the results of the realistic model and the results of the simplified model confirm the importance of including accurate models of the actual antennas in GPR simulations; they also emphasize how salient it is to remove antenna effects as a pre-processing step of experimental GPR data. The simulation results of the antenna over the concrete cell presented in this paper are attached to the paper as ‘Supplementary materials.’

KEYWORDS: Ground Penetrating Radar (GPR); Electromagnetic modelling; Finite-Integration technique (FIT); Antennas; TU1208 Open Database of Radargrams; concrete.

1. INTRODUCTION

Electromagnetic simulations of Ground Penetrating Radar (GPR) [1] scenarios including realistic models of the antennas are not yet common. Accurate models of GPR antennas have been only occasionally developed during the past two decades [2]-[9]; rarely, they have been combined with realistic models of complex environments [10]. In most cases, GPR electromagnetic simulations use hertzian dipoles or lines of current to represent the transmitting antennas; the physical structure of the receiving antennas is usually not included in the models and the electric field impinging on the receivers is calculated [11]-[16]. This simplified approach is customarily adopted because easier to implement and computationally cheaper; in fact, nowadays running realistic models of GPR scenarios is still a challenging task, notwithstanding computing power is increasing and becoming more accessible.

In this paper, we employed commercial software implementing the Finite-Integration technique (FIT) [17] (CST Microwave Studio) for modelling and simulating an antenna representative of a widely used high-frequency commercial device manufactured by Geophysical Survey Systems, Inc. (GSSI). All necessary information about the antenna was taken from Dr Craig Warren's PhD Thesis [6], where the freeware tool GprMax3D [18] was used to develop a Finite-Difference Time-Domain (FDTD) model of the same antenna. It has to be noted that, in [6] and here, the numerical model does not exactly replicate the commercial antenna because the electromagnetic properties of some antenna materials are unknown, due to commercial sensitivity; the undisclosed values were estimated in [6] (the match between the real and synthetic crosstalk responses of the antenna in free-space was maximized, by using Taguchi's optimisation method). It is also worth mentioning that the FDTD model developed in [6] is currently included in the library of antennas of the open-source software gprMax [19, 20], therefore gprMax users can easily include this antenna into their simulations without having to build it step-by-step. The CST model that we developed was successfully validated via comparisons with synthetic and experimental data available in [6], in cooperation with colleagues from The University of Edinburgh (United Kingdom); such data were obtained with the antenna immersed in free space and in lossy dielectric environments, with and without a circular-section metallic target and some results of the performed comparisons were presented in a conference paper [21].

In Section 2 of the present paper, we describe in detail how we developed the CST Microwave Studio model of the antenna; this information was not included in [21]. Then, in Section 3, we present new results that we obtained by simulating the antenna over a reinforced-concrete cell. Such cell is one of the reference scenarios included in the Open Database of Radargrams of COST Action TU1208 [22] and hosts a series of five circular-section steel rods, having different diameters and/or embedded at different depths into the concrete [23]. We compare results obtained by using the realistic CST antenna model, and results obtained by representing the transmitting antenna with a line of current and by neglecting the physical structure of the receiving antenna. The aim of this comparison is to confirm and further highlight the importance of including realistic models of the actual antennas in GPR simulations, whenever the objective of the simulations is to accurately replicate a real GPR response, or to exploit the simulation results into an inversion process. Moreover, the comparisons presented in this paper emphasize once more how strong are antenna effects, and therefore, how salient it is to develop methods for removing them as a pre-processing step of GPR data. The results of our simulations are attached to the paper as ‘Supplementary materials.’

3. BUILDING THE CST MICROWAVE STUDIO MODEL OF THE ANTENNA

We used CST Microwave Studio to simulate an antenna representative of the 1.5 GHz (Model 5100) device manufactured by GSSI, which is a high-frequency high-resolution antenna using bowties as transmitting and receiving elements. As already mentioned in the Introduction, all information about the electromagnetic and geometrical properties of the antenna was taken from Dr Craig Warren’s PhD Thesis [6].

The bowtie is a compact, light and cheap to produce broadband antenna, which is very often used in GPR systems [24]. The bowtie size and flare angle are critical to the performance of the antenna. The bowties simulated in this paper have a flare angle of 76° , with rectangular patches added to their open ends (these extensions introduce a delay in the signal path and create destructive interference patterns that reduce unwanted resonance phenomena); the triangle base and height are 22 mm and 15 mm long, respectively; the size of the additional rectangular patches is 22 mm \times 14 mm (see Figure 1).

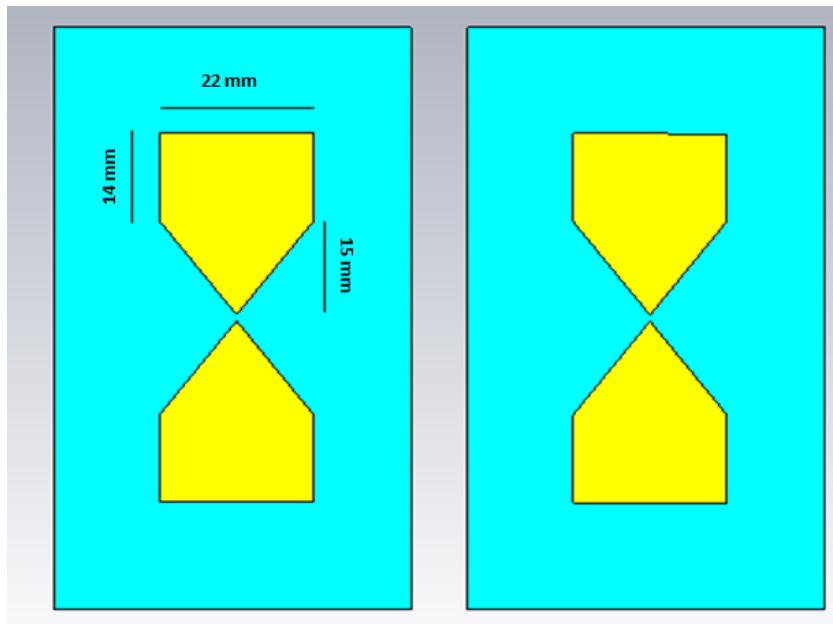


FIG. 1 – Geometrical sketch of the simulated bowties.

The simulated bowties are etched from 1-mm thick copper onto Printed Circuit Boards (PCB); they are enclosed in glass fibre boxes and then in rectangular metal boxes, which act as shields (shields are important to prevent electromagnetic emissions from the antenna interfering with surrounding electronic equipment, as well as to reduce the exposure of the human operator to the electromagnetic fields). Open-cell carbon-loaded foam is used, which acts as a broadband electromagnetic absorber to reduce unwanted resonance in the cavities behind the transmitting and receiving bowties. Some components of the GSSI antenna are made from plastics: in particular, the enclosure of the overall antenna is made of polypropylene (PP) and the 2-mm thick skid plate is made of High-Density Polyethylene (HDPE) (the skid plate is a replaceable component designed to protect the base of the antenna from damage).

In CST Microwave Studio, we modelled the shields and any other metallic components as perfectly conducting (PEC), apart from the bowties. Indeed, for the copper bowties we assumed a constant relative permittivity $\epsilon_{\text{copper}} = 1$ and a conductivity $\sigma_{\text{copper}} = 59.6 \cdot 10^6 \text{ S/m}$ (same as in [6]).

For the plastics, all values were taken from [6]. In particular, for the HDPE skid plates, for the PP case, and for the glass fibre of the PCB, the following constant relative permittivity values were used: $\epsilon_{\text{HDPE}} = 2.35$, $\epsilon_{\text{PP}} = 2.26$, and $\epsilon_{\text{PCB}} = 3$, respectively; moreover, losses were neglected ($\sigma_{\text{HDPE}} = \sigma_{\text{PP}} = \sigma_{\text{PCB}} = 0$). The electromagnetic properties of the absorbers are unknown, for commercial reasons; the following values were estimated in [6] via comparisons between experimental and synthetic results: $\epsilon_{\text{abs}} = 6.49$ and $\sigma_{\text{abs}} = 0.252$ S/m. We used the same values in our CST models.

In Figure 2, geometrical sketches are reported, to better clarify the geometry of the modelled device and the size of all its parts (such sketches are generated by the computer-aided drafting tool of CST); a photo of the real antenna can be found in Fig. 24 of [6].

In the real antenna, the transmitter and receiver bowties are connected to circuits that generate the input pulses and process the received signals. The physical electronic components of these circuits were not modelled in [6] and also here, for two reasons: because the circuit design and components properties are unknown; and, because to accurately model components of that size a sub-millimetre mesh should be used, which would increase the computational requirements. In CST, for the receiver circuitry of both antennas we used a lumped resistance in the gap between the receiver bowtie arms. The software offers the possibility to insert simple electronic components in the model, called 'Lumped Network Elements' (LEMs). Three different circuits can be used: RLC-Serial, RLC-Parallel and Diode: see Figure 3(a)-(c). Obviously, it is possible to model sub-circuits of these RLC circuits by setting one or more components to 0 (this removes the respective components from the circuit). In [6], resistance components were modelled by specifying the corresponding conductivity of a single-cell edge. Although we adopted in our models the same value as in [6] for the resistance at the receiver, i.e., $R_{\text{Rx}} = 925 \Omega$, it has to be kept in mind that the resistance is modelled differently in GprMax3D and CST, which may cause small differences in the results. For what concerns the feeding, CST provides three different source elements to excite a model: 'waveguide ports', 'plane waves', and 'discrete ports' ('edge' and 'face'). We opted for a discrete face port to simulate a lumped element source. Three different discrete face ports are available in CST, where the excitation is considered as a voltage, as current source, or as an

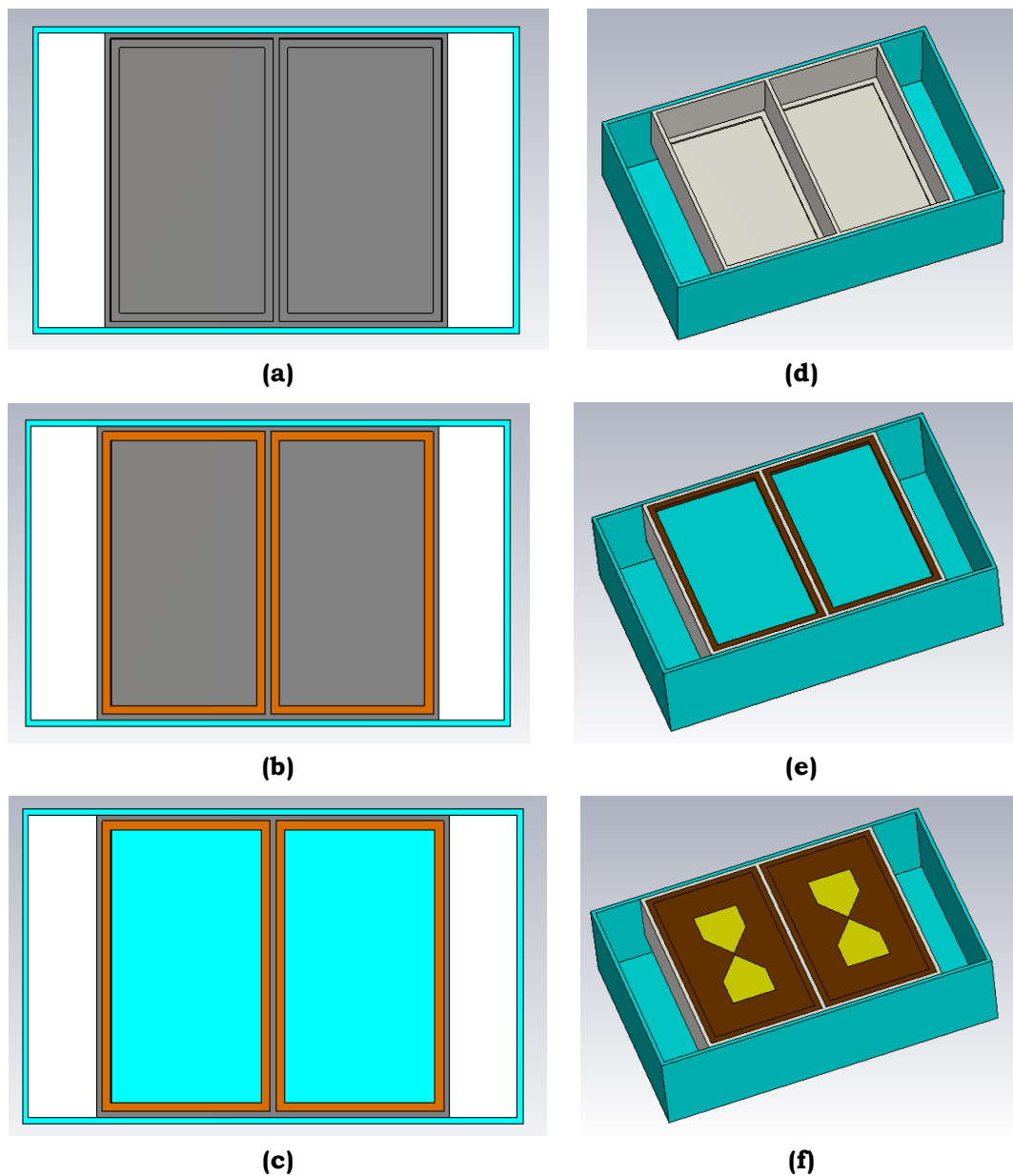


FIG. 2 – Geometrical sketches of antenna parts: **(a)** PP enclosure (170 mm × 107 mm × 43 mm; the PP thickness is 2 mm) and metal shielding structure (120 mm × 103 mm × 27 mm; PEC thickness is 2 mm); **(b)** PP enclosure, metal shielding structure and two glass fibre boxes (57 mm × 99 mm × 24 mm; the glass fibre thickness is 3 mm); **(c)** PP enclosure, metal shielding structure, glass fibre boxes and microwave absorbers (51 mm × 93 mm × 23 mm), on which the antennas sketched in Figure 1 are finally placed; **(d)** PP enclosure and metal shielding structure; **(e)** PP enclosure, metal shielding structure, glass fibre boxes and microwave absorbers; **(f)** the whole antenna structure, with bowties embedded in PCB.

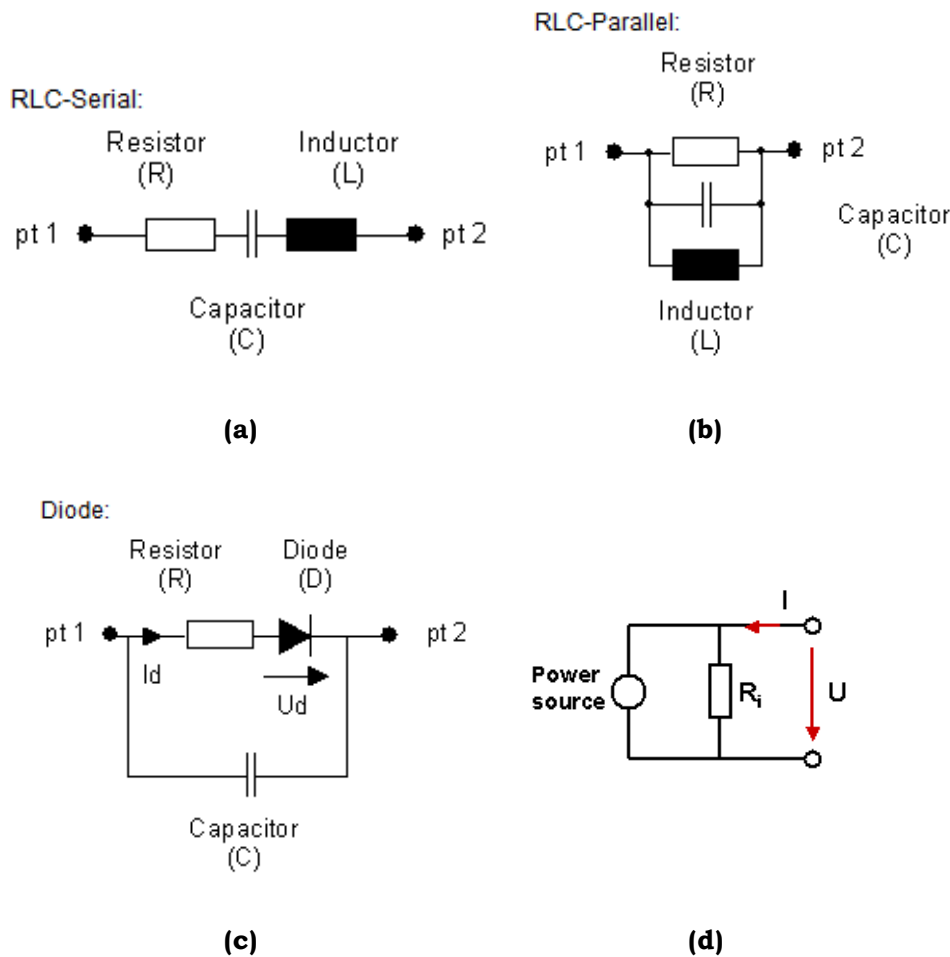


FIG. 3 – **(a)-(c)** Lumped Network Elements available in CST; **(d)**: Equivalent circuit of the CST S-parameter discrete face port.

impedance element that also absorbs some power and enables S-parameter calculation; we used the latter, which equivalent circuit is shown in Figure 3(d). The resistance at the drive point was $R_{Tx} = 10 \text{ k}\Omega$, whereas in [6] the optimized value of the drive-point resistance was $4 \text{ }\Omega$ because a different feeding model was used (with series instead of parallel resistance). We estimated the best value of our resistance in an empiric way: we performed several simulations and compared the CST crosstalk response of the antenna in a vacuum with the GprMax3D response taken from [6]; then, we adopted the resistance value that provided the best agreement.

Concerning the shape and frequency content of the emitted pulse, those used by GSSI are unknown parameters; in [6], it was decided to use a Gaussian pulse because this is a common choice in GPR simulations. The expression of the Gaussian pulse of unit amplitude is:

$$V_G(t) = \exp[-2\pi^2 f^2 (t - 1/f)^2] \quad (1)$$

where f is the pulse centre frequency and t is the time. The first derivative with respect to time of the Gaussian pulse is often used in GPR simulations, too:

$$V_{DG}(t) = -4\pi^2 f^2 \exp[-2\pi^2 f^2 (t - 1/f)^2] (t - 1/f) \quad (2)$$

A centre frequency equal to 1.71 GHz (different than the frequency stated by the manufacturer) was identified in [6] by measuring the crosstalk response of the real antenna. With this value of the centre frequency, the amplitude of the pulses (1) and (2) is plotted versus time in Figure 4(a); the spectral content of the pulses is shown in Figure 4(b). By comparing the time shape of the Gaussian pulse with the curves in Figure 3 of [21], it is already clear that the antenna structure has a strong influence on the signal recorded by a GPR. For all results presented in the following Section, the emitted pulse shape was Gaussian and the centre frequency was 1.71 GHz.

3. NUMERICAL RESULTS

The CST model that we developed was validated via comparisons with synthetic and experimental data available in [6], in cooperation with our colleagues from The University of Edinburgh; the considered data were obtained with the antenna in free space and over lossy half-spaces (emulsions), with and without a circular-section metallic target; the achieved agreement was very good and some comparisons were presented in the conference paper [21].

In this Section, we present new results obtained by simulating the antenna over a reinforced-concrete cell hosting five circular-section steel rods with different diameters and/or burial depths. This cell was first proposed in [23] and its cross-section is shown in Figure 5. In the simulations, the relative permittivity of concrete is 6 and its conductivity is 0.01 S/m; the relative permittivity of the compacted fill is 16 and its conductivity is 0.005 S/m; the circular-section cylinders

embedded in concrete are assumed to be PEC. Results are calculated in five different positions, namely with the center of the overall antenna above the axes of the five targets; the bowtie axes are always parallel to the axes of the cylinders.

We also used GprMax2D to implement and execute a simplified two-dimensional model of the same scenario, where the transmitting antenna is represented by a line source, the receiving antenna is not modelled, and the electric field impinging on the receiver is calculated. As already mentioned in the Introduction, this kind of simplified simulation is most often found in the GPR scientific literature, because easier to implement and less demanding from a computational point of view than the simulation of a realistic three-dimensional model.

In Figure 6, the amplitude of the signal received by the GPR is plotted as a function of time when the antenna is positioned above the cylinder having a 2-cm diameter and buried at 6 cm from the air-concrete interface (i.e., the first cylinder starting from the left in Figure 5); CST results for the realistic model and GprMax2D results for the simplified model are shown, and both curves have been normalized to their absolute maximum value for a better readability of the comparison. In Figure 7, the same is shown when the antenna is above the cylinder having a 2-cm diameter and buried at 9 cm from the air-concrete interface (i.e., the second cylinder starting from the left in Figure 5). Analogously, in Figure 8 the same is shown when the antenna is above the cylinder having a 2-cm diameter and buried at 12 cm from the air-concrete interface (i.e., the third cylinder starting from the left in Figure 5). In Figure 9, the same is shown when the antenna is above the cylinder having a 1-cm diameter and buried at 9 cm from the air-concrete interface (i.e., the fourth cylinder starting from the left in Figure 5). And, in Figure 10 the same is shown when the antenna is above the largest cylinder having a 3 cm diameter and buried at 9 cm from the air-concrete interface (i.e., the fifth and last cylinder starting from the left in Figure 5).

To ease the Reader's comprehension and interpretation of the curves presented in Figures 6-10, in Figure 11 a synthetic B-Scan is reported, which was obtained by moving the antenna above the entire concrete cell, with a 5 mm spatial step (this B-Scan was calculated by using GprMax2D, for the simplified model).

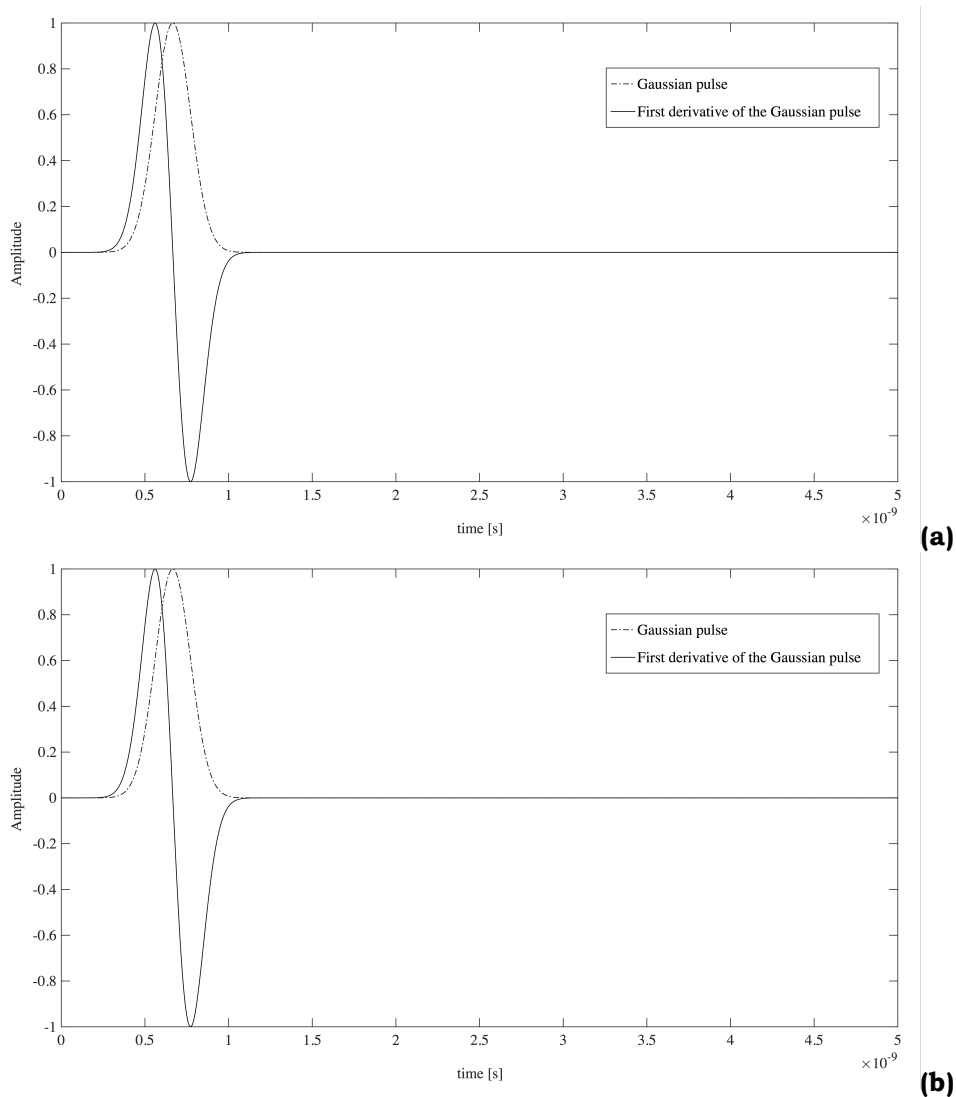


FIG. 4 – (a) Amplitude (a.u.) of the pulses (1) and (2) versus time; (b) single-sided spectrum of the pulses (1) and (2) (a.u.). In the simulations presented in this paper, a Gaussian pulse is used.

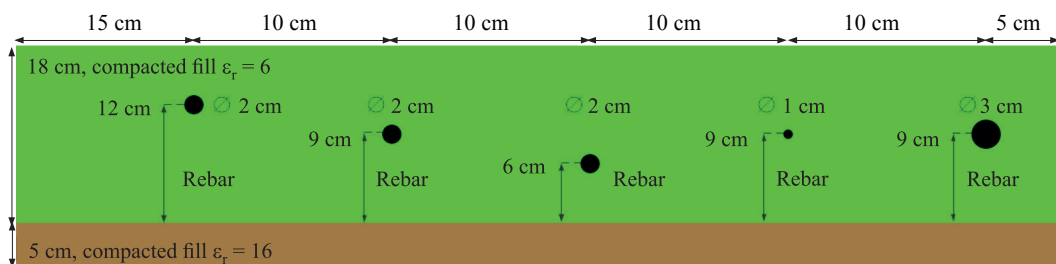


FIG. 5 – Geometry of the concrete cell proposed in [23].

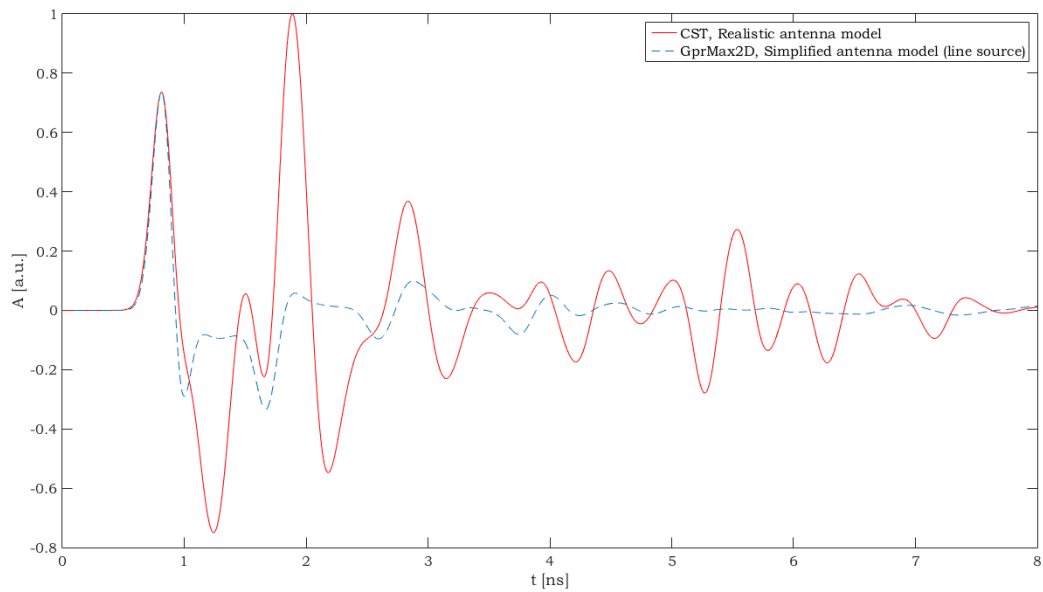


FIG. 6 – Amplitude of the signal received by the GPR, normalized to its absolute maximum value, as a function of time; the antenna is positioned above the cylinder having a 2-cm diameter and buried at 6 cm from the air-concrete interface.

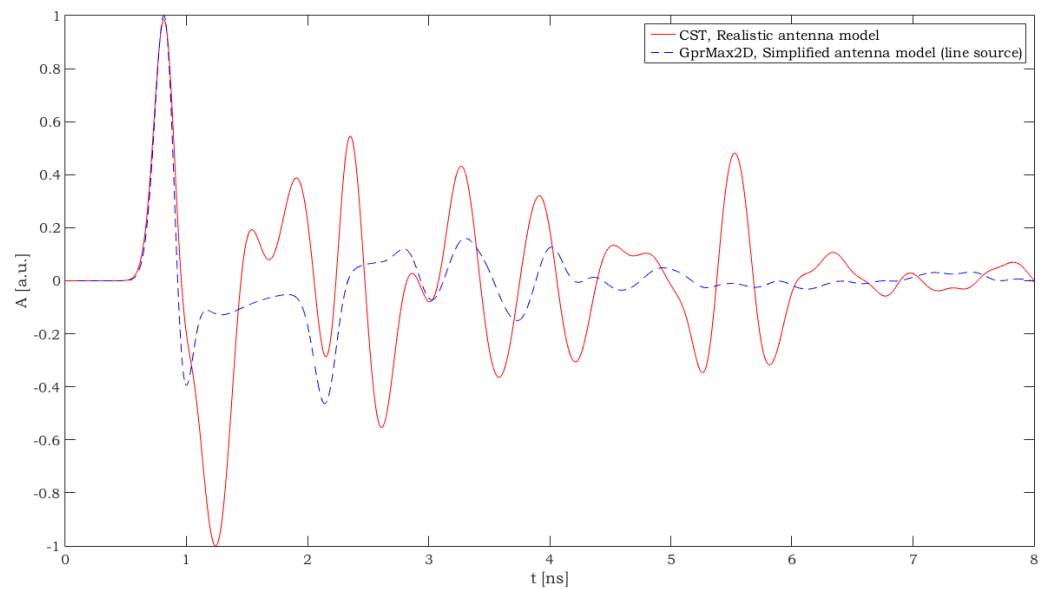


FIG. 7 – Same as in Fig. 6, when the antenna is positioned above the cylinder having a 2-cm diameter and buried at 9 cm from the air-concrete interface.

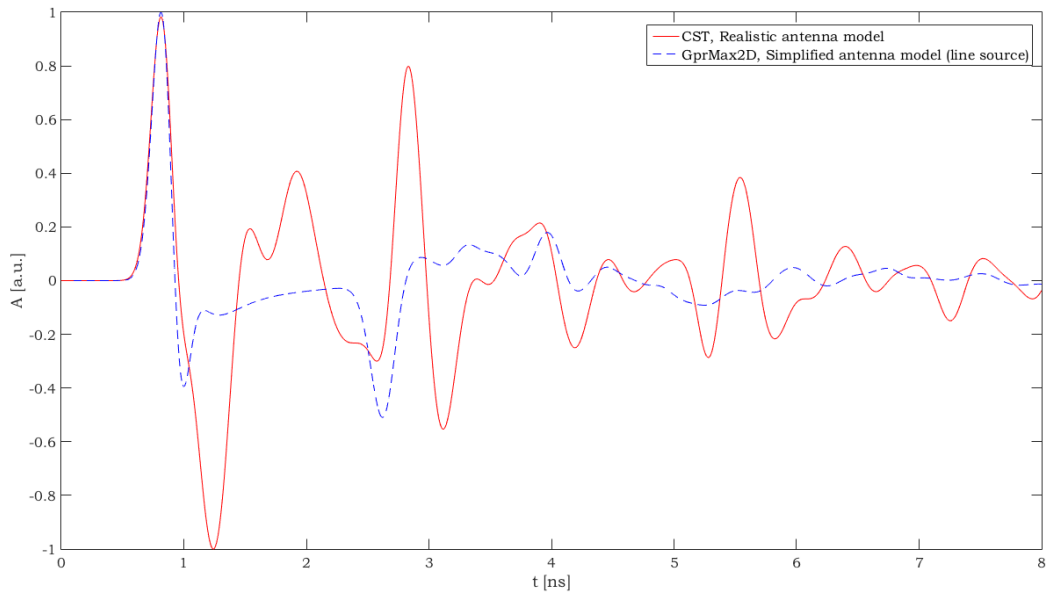


FIG. 8 – Same as in Fig. 6, when the antenna is positioned above the cylinder having a 2-cm diameter and buried at 12 cm from the air-concrete interface.

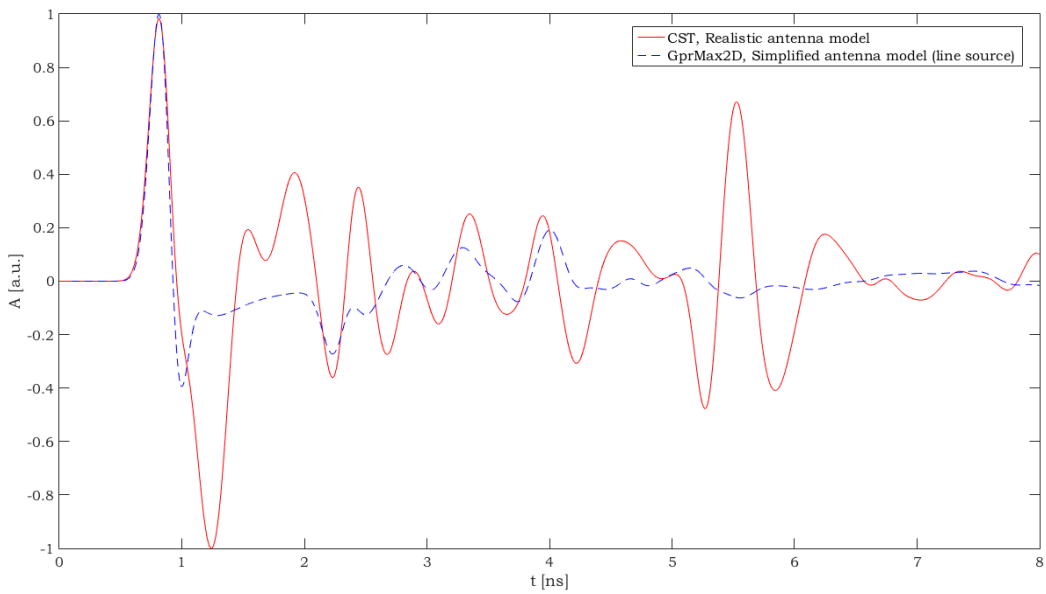


FIG. 9 – Same as in Fig. 6, when the antenna is positioned above the cylinder having a 1-cm diameter and buried at 9 cm from the air-concrete interface.

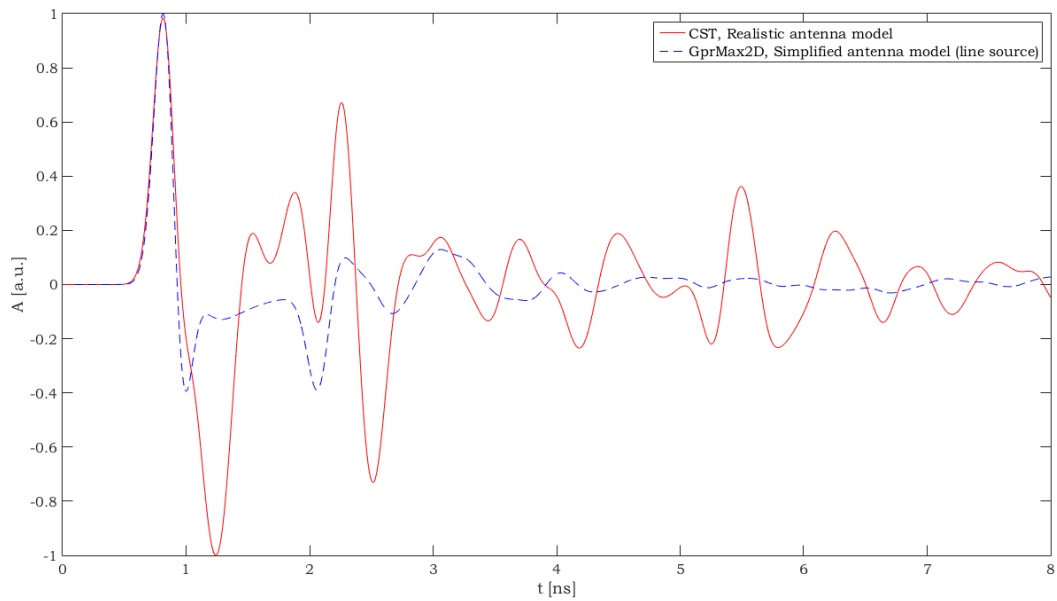


FIG. 10 – Same as in Fig. 6, when the antenna is positioned above the cylinder having a 3-cm diameter and buried at 9 cm from the air-concrete interface.

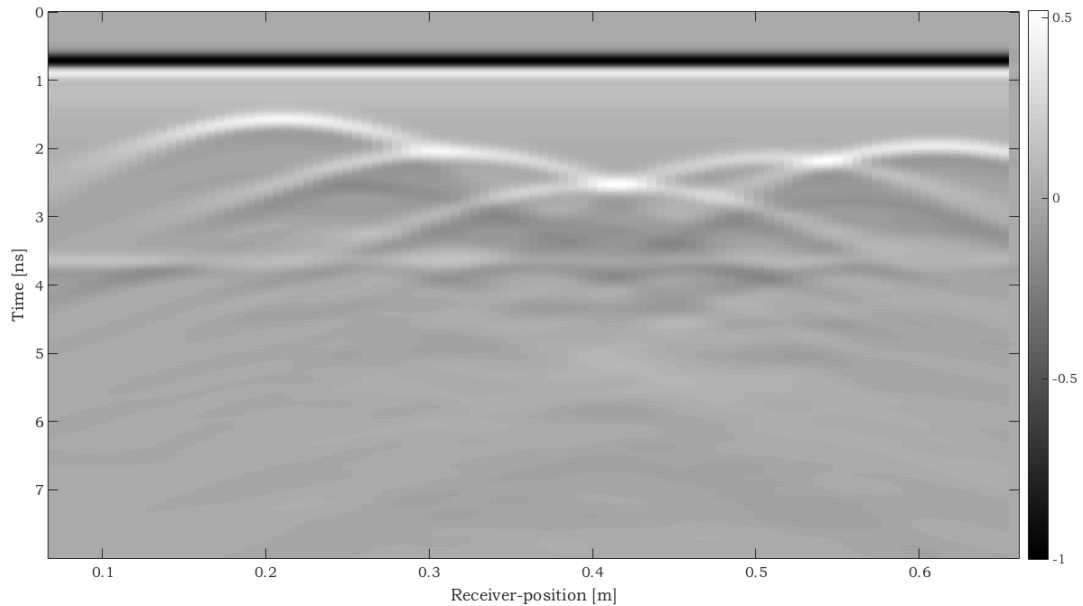


FIG. 11 – B-Scan obtained by moving the GPR antenna above the entire concrete cell, with a 5 mm spatial step (GprMax2D results for the simplified model).

From Figures 6-10, it is apparent that the differences between the simulation results of the realistic model and those of the simplified model are significant. It can be noticed that, in many cases, the arrival time of echoes coming from the targets are in good agreement (the worst agreement is in Figure 8, when the antennas are in the middle of the scenario and the electromagnetic interactions between the targets are stronger). The amplitude and shape of the various echoes, instead, are highly different for the two models.

The presented comparisons confirm that for an accurate simulation of GPR scenarios (i.e., for obtaining a synthetic response close to the real one) it is crucial to develop detailed and unidealized models, not only of the environment (surveyed ground or structure and targets) but also of the antennas, which makes absolutely sense, because the antennas strongly affect the responses recorded by the radar.

Furthermore, the comparisons shown in this paper emphasize how salient it is to filter out the antenna effects as a pre-processing step of GPR data, whenever GPR data wish to be used not only for estimating the depth of interfaces and targets (from the arrival instants of the relevant echoes) but also for assessing other geometrical and physical properties, such as the size and relative permittivity of targets (by analyzing the amplitude and shape of the various echoes) [25], [26]. Prominent efforts are being done in this sense; a Belgian research team recently developed a novel approach for the removal of antenna effects [27], [28], which allows filtering out the antenna multiple internal reflections, the antenna-medium ringing, and the antenna height variation effects from GPR data acquired in near-field conditions above a locally multilayered medium.

4. CONCLUSIONS

Realistic models of Ground-Penetrating Radar (GPR) antennas in complex environments are not common in the scientific literature. In this paper, a full-wave electromagnetic model of a high-frequency GPR antenna over a concrete cell with reinforcing elements was implemented by using the commercial software CST Microwave Studio, which makes use of the Finite-Integration technique. The simulated antenna is representative of a 1.5 GHz device manufactured by Geophysical Survey

Systems, Inc. All information to build the antenna model was taken from the PhD thesis of Dr Craig Warren [6], where the same device was simulated for the first time by using the well-known Finite-Difference Time-Domain software GprMax3D; our exercise was possible because [6] is very clearly written and all steps are explained in an exhaustive way. The simulated concrete cell with reinforcing elements is one of the reference scenarios included in the Open Database of Radargrams of COST Action TU1208 “Civil engineering applications of Ground Penetrating Radar” and hosts five circular-section steel rods, having different diameters, embedded at different depths into the concrete [23].

In Section 2 of this paper, the implementation of the CST Microwave Studio antenna model was described in detail.

In Section 3, new results calculated with the antenna over the above-mentioned concrete cell were presented. Comparisons with a simpler model, where the physical structure of the antenna was not taken into account, were carried out. The aim of such comparisons was to confirm and further highlight the importance of including realistic models of the actual antennas in GPR simulations, whenever the objective of the simulations is to replicate the real GPR response or to exploit the forward-scattering results into an inversion process. This is especially true when GPR is used for locating and identifying shallow targets in a heterogeneous environment (e.g., landmines in the soil) or multiple closely separated targets embedded at a limited depth in a structure (e.g., reinforcing elements, voids and cracks in concrete). For such applications, high-frequency antennas are used, to achieve sufficient resolution; the responses from the sought targets arrive at the receiving antenna very soon and are often superimposed between each other, moreover strong electromagnetic interactions between targets, as well as between antennas and targets, take place (therefore, the recorded responses strongly depend on the properties of the transmitting and receiving antennas). The comparisons presented in this paper are also a reminder of how salient it is to remove antenna effects as a pre-processing step of GPR data; additionally, they show how the simulation of simplified models can be useful to aid the interpretation of experimental responses (and of synthetic responses generated by executing more complex models).

An archive containing the results of the simulations of the antenna over the reinforced concrete cell are attached to this paper as

‘Supplementary materials’. Reproducing these results may be a useful exercise for a University student who wishes to learn how to use an electromagnetic simulator; actually, the work presented herein was mostly developed during the Master thesis in Electronic Engineering of the first author, under the supervision of the second author.

ACKNOWLEDGEMENTS

The work presented in this paper was carried out as a contribution to COST (European Cooperation in Science and Technology) Action TU1208 “Civil Engineering Application of Ground Penetrating Radar”. The authors are grateful to COST for funding and supporting COST Action TU1208.

SUPPLEMENTARY MATERIALS

Data presented in Figures 7-12 can be downloaded at the following url:

http://gpradar.eu/onewebmedia/SupplementaryMaterials_GPR-1-2-3.zip

REFERENCES

- [1] A. Benedetto and L. Pajewski, Eds. “Civil Engineering Applications of Ground Penetrating Radar,” Publishing House: Springer International; Book Series "Springer Transactions in Civil and Environmental Engineering;" April 2015; e-book ISBN: 9783319048130; hardcover ISBN: 9783319048123; doi: 10.1007/9783319048130; 371 pp.
- [2] L. Gurel and U. Oguz, “Three-dimensional FDTD modeling of a Ground-Penetrating Radar,” *IEEE Transactions on Geoscience and Remote Sensing*, vol. 38, no. 4, pp. 1513–1521, July 2000, doi: 10.1109/36.851951.
- [3] S. Lambot, E. C. Slob, I. van den Bosch, B. Stockbroeckx, and M. Vanclooster, “Modeling of Ground-Penetrating Radar for accurate characterization of subsurface electric properties,” *IEEE Transactions on Geoscience and Remote Sensing*, vol. 42, no. 11, pp. 2555–2568, November 2004, doi: 10.1109/TGRS.2004.834800.
- [4] G. Klysz, X. Ferrieres, J. Balayssac, and S. Laurens, “Simulation of direct wave propagation by numerical FDTD for a GPR coupled antenna,” *NDT & E International*, vol. 39, no. 4, pp. 338–347, November 2006, doi: 10.1016/j.ndteint.2005.10.001.

- [5] A. Ahmed, Y. Zhang, D. Burns, D. Huston, and T. Xia, "Design of UWB Antenna for Air-Coupled Impulse Ground-Penetrating Radar," *IEEE Geoscience and Remote Sensing Letters*, vol. 13, no. 1, pp. 92–96, January 2016, doi: 10.1109/LGRS.2015.2498404.
- [6] C. Warren, "Numerical modelling of high-frequency ground-penetrating radar antennas," PhD Thesis, The University of Edinburgh, 2009 (available for download at <http://hdl.handle.net/1842/4074> - last checked 2 July 2018).
- [7] C. Warren and A. Giannopoulos, "Creating FDTD models of commercial GPR antennas using Taguchi's optimisation method," *Geophysics*, vol. 76, no. 2, pp. G37–G47, March 2011, doi: 10.1190/1.3548506.
- [8] N. Diamanti and A. P. Annan, "Characterizing the energy distribution around GPR antennas," *Journal of Applied Geophysics*, vol. 99, pp. 83–90, December 2013, doi: 10.1016/j.jappgeo.2013.08.001.
- [9] C. Warren and A. Giannopoulos, "Experimental and Modeled Performance of a Ground Penetrating Radar Antenna in Lossy Dielectrics," *IEEE Journal of Selected Topics in Applied Earth Observations and Remote Sensing*, vol. 9, no. 1, pp. 29–36, Jan. 2016, doi: 10.1109/JSTARS.2015.2430933.
- [10] I. Giannakis, A. Giannopoulos, and C. Warren, "A Realistic FDTD Numerical Modeling Framework of Ground Penetrating Radar for Landmine Detection," *IEEE Journal of Selected Topics in Applied Earth Observations and Remote Sensing*, vol. 9, no. 1, pp. 37–51, January 2016, doi: 10.1109/JSTARS.2015.2468597.
- [11] A. Benedetto, F. Tosti, L. Pajewski, F. D'Amico, and W. Kusayanagi, "FDTD Simulation of the GPR Signal for Effective Inspection of Pavement Damages," *Proceedings of the 15th International Conference on Ground Penetrating Radar (GPR 2014)*, Brussels, Belgium, 30 June – 4 July 2014, pp. 513–518, doi: 10.1109/ICGPR.2014.6970477.
- [12] P. Shanguan and I. L. Al-Qadi, "Calibration of FDTD Simulation of GPR Signal for Asphalt Pavement Compaction Monitoring," *IEEE Transactions on Geoscience and Remote Sensing*, vol. 53, no. 3, pp. 1538–1548, March 2015, doi: 10.1109/TGRS.2014.2344858.
- [13] M. Solla, R. Asorey-Cacheda, X. Núñez-Nieto, and B. Conde-Carnero, "Evaluation of historical bridges through recreation of GPR models with the FDTD algorithm," *Construction and Building Materials*, vol. 77, pp. 19–27, January 2016, doi: 10.1016/j.ndteint.2015.09.003.
- [14] M. Loewer and J. Igel, "FDTD simulation of GPR with a realistic multi-pole debye description of lossy and dispersive media," *Proceedings of the 16th International Conference on Ground Penetrating Radar (GPR 2016)*, Hong Kong, 13– 6 June 2016, pp. 1–5, doi: 10.1109/ICGPR.2016.7572599.

- [15] J. Igel, S. Stadler, and T. Günther, “High-resolution investigation of the capillary transition zone and its influence on GPR signatures,” Proceedings of the 16th International Conference on Ground Penetrating Radar (GPR 2016), Hong Kong, 13–16 June 2016, pp. 1–5, doi: 10.1109/ICGPR.2016.7572603.
- [16] A. Benedetto, F. Tosti, L. Bianchini Ciampoli, A. Calvi, M. G. Brancadoro, and A. M. Alani, “Railway ballast condition assessment using ground-penetrating radar – An experimental, numerical simulation and modelling development,” *Construction and Building Materials*, vol. 140, pp. 508–520, June 2017, doi: 10.1016/j.conbuildmat.2017.02.110.
- [17] T. Weiland, “A discretization model for the solution of maxwell’s equations for six-component fields,” *Archiv Elektronik und Uebertragungstechnik*, vol. 31, pp. 116–120, 1977.
- [18] A. Giannopoulos, “Modelling ground penetrating radar by GprMax,” *Construction and building materials*, vol. 19, no. 10, pp. 755–762, December 2005, doi: 10.1016/j.conbuildmat.2005.06.007.
- [19] C. Warren, A. Giannopoulos, and I. Giannakis, “gprMax: Open source software to simulate electromagnetic wave propagation for Ground Penetrating Radar,” *Computer Physics Communications*, vol. 209, pp. 163–170, December 2016, doi: 10.1016/j.cpc.2016.08.020.
- [20] C. Warren, A. Giannopoulos, N. Diamanti, and P. Annan, “An extension module to embed commercially sensitive antenna models in gprMax,” Proceedings of the 8th International Workshop on Advanced Ground Penetrating Radar (IWAGPR 2015), 7–10 July 2015, Florence, Italy, pp. 1–3, doi: 10.1109/IWAGPR.2015.7292623.
- [21] C. Warren, L. Pajewski, A. Ventura, and A. Giannopoulos, “An Evaluation of Finite-Difference and Finite-Integration Time-Domain Modelling Tools for Ground Penetrating Radar Antennas,” Proceedings of the 10th European Conference on Antennas and Propagation (EuCAP 2016), 10–15 April 2016, Davos, Switzerland, pp. 1–5, doi: 10.1109/EuCAP.2016.7482010.
- [22] X. Dérobert and L. Pajewski, “TU1208 Open Database of Radargrams: The Dataset of the IFSTTAR Geophysical Test Site,” *Remote Sensing*, vol. 10, article ID 530, pp. 1–50, March 2018, doi: 10.3390/rs10040530.
- [23] L. Pajewski and A. Giannopoulos, “Electromagnetic Modelling of Ground Penetrating Radar Responses to Complex Targets,” Short Term Scientific Missions and Training Schools – Year 1, COST Action TU1208, L. Pajewski & M. Marciniak, Eds., Aracne Editrice, Rome, Italy, May 2014, ISBN 9788854872257, pp. 7–45 (available for download at www.GPRadar.eu).
- [24] L. Pajewski, F. Tosti, and W. Kusayanagi, “Antennas for GPR Systems,” Chapter 2 in A. Benedetto and L. Pajewski, Eds. “Civil Engineering

Applications of Ground Penetrating Radar,” Publishing House: Springer International; Book Series "Springer Transactions in Civil and Environmental Engineering;" April 2015; e-book ISBN: 9783319048130; hardcover ISBN: 9783319048123; doi: 10.1007/9783319048130; 371 pp.

[25] F. Frezza, P. Martinelli, L. Pajewski, and G. Schettini, “A CWA-Based Detection Procedure of a Perfectly-Conducting Cylinder Buried in a Dielectric Half-Space,” Progress In Electromagnetics Research B, vol. 7, 265–280, 2008, doi: 10.2528/PIERB08032603.

[26] F. Frezza, P. Martinelli, L. Pajewski, and G. Schettini, “Short-Pulse Electromagnetic Scattering by Buried Perfectly Conducting Cylinders,” IEEE Geoscience and Remote Sensing Letters, vol. 4, no. 4, pp. 611–615, October 2007, doi: 10.1109/LGRS.2007.903078.

[27] A. De Coster and S. Lambot, “Full-wave removal of internal antenna effects and antenna-medium coupling for improved ground-penetrating radar,” IEEE Transactions on Geoscience and Remote Sensing, Submitted (TGRS-2018-00050).

[28] A. De Coster and S. Lambot, “Fusion of Multifrequency GPR Data Freed From Antenna Effects,” in IEEE Journal of Selected Topics in Applied Earth Observations and Remote Sensing, vol. 11, no. 2, pp. 664-674, February 2018, doi: 10.1109/JSTARS.2018.2790419.

The scientific paper that you have downloaded is included in Issue 2, Volume 1 (July 2018) of the journal *Ground Penetrating Radar* (ISSN 2533-3100; journal homepage: www.gpradar.eu/journal).

All *Ground Penetrating Radar* papers are processed and published in true open access, free to both Authors and Readers, thanks to the generous support of TU1208 GPR Association and to the voluntary efforts of the journal Editorial Board. The publication of Issue 2, Volume 1 is also supported by Adapis Georadar Teknik Ab (georadar.eu) and by IDS Georadar s.r.l. (idsgeoradar.com).

The present information sheet is obviously not part of the scientific paper.

